UC Santa Barbara
UC Santa Barbara Previously Published Works

Title

Ontogeny of Circadian Rhythms and Synchrony in the Suprachiasmatic Nucleus

Permalink

Journal

ISSN

Authors

Carmona-Alcocer, Vania
Abel, John H
Sun, Tao C
et al.

Publication Date

DOI

Peer reviewed

Ontogeny of circadian rhythms and synchrony in the suprachiasmatic nucleus

Vania Carmona-Alcocer[1], John H. Abel[2], Tao C. Sun[1],
Linda R. Petzold[3], Francis J. Doyle III[4], Carrie L. Simms[1] and Erik D. Herzog[1,*]

[1]Department of Biology, Washington University in St. Louis, St. Louis, Missouri 63130-4899
[2]Department of Systems Biology, Harvard Medical School, Boston, Massachusetts 02115
[3]Department of Computer Science, University of California, Santa Barbara, Santa Barbara, California 93106
[4]John A. Paulson School of Engineering and Applied Sciences, Harvard University, Cambridge, Massachusetts 02138

[*]Corresponding author: Erik D. Herzog
Email: herzog@wustl.edu
Phone: +1 314-935-8635
Full address: Department of Biology Box 1137, Washington University, St. Louis, MO 63130-4899

July 2017

Classification:
Biological Science | Neuroscience | Development

Keywords:
Clock genes | Ontogeny | VIP

Author contributions:
Designed research: C.L.S., E.D.H., V.C.A
Performed research: V.C.A., T.C.S., C.L.S.
Analyzed Data: V.C.A., J.H.A., L.R.P., F.J.D., E.D.H.,
Wrote the Paper: V.C.A, J.H.A., E.D.H.

Abstract

In mammals, the suprachiasmatic nucleus (SCN) of the hypothalamus coordinates daily rhythms including sleep-wake, hormone release and gene expression. The cells of the SCN must synchronize to each other to drive these circadian rhythms in the rest of the body. The ontogeny of circadian cycling and intercellular coupling in the SCN remains poorly understood. Recent *in vitro* studies have recorded circadian rhythms from the whole embryonic SCN. Here, we tracked the onset and precision of rhythms in PERIOD2 (PER2), a clock protein, within the SCN isolated from embryonic and postnatal mice of undetermined sex. We found that a few SCN cells developed circadian periodicity in PER2 by 14.5 days after mating (E14.5) with no evidence for daily cycling on E13.5. On E15.5, the fraction of competent oscillators increased dramatically corresponding with stabilization of their circadian periods. The cells of the SCN harvested at E15.5 expressed sustained, synchronous daily rhythms. By postnatal day 2 (P2), SCN oscillators displayed the daily, dorsal-ventral phase wave in clock gene expression typical of the adult SCN. Strikingly, vasoactive intestinal polypeptide (VIP), a neuropeptide critical for synchrony in the adult SCN, and its receptor, VPAC2R, reached detectable levels after birth and after the onset of circadian synchrony. Antagonists of GABA or VIP signaling or action potentials did not disrupt circadian synchrony in the E15.5 SCN. We conclude that endogenous daily rhythms in the fetal SCN begin with few noisy oscillators on E14.5, followed by widespread oscillations that rapidly synchronize on E15.5 by an unknown mechanism.

Significance Statement

We recorded the onset of PER2 circadian oscillations during embryonic development in the mouse SCN. When isolated at E13.5, the anlagen of the SCN expresses high, arrhythmic PER2. In contrast, a few cells show noisy circadian rhythms in the isolated E14.5 SCN and most show reliable, self-sustained, synchronized rhythms in the E15.5 SCN. Strikingly, this synchrony at E15.5 appears prior to expression of VIP or its receptor and persists in the presence of blockers of VIP, GABA or neuronal firing. Finally, the dorsal-ventral phase wave of PER2 typical of the adult SCN appears around P2, indicating that multiple signals may mediate circadian synchrony during the ontogeny of the SCN.

Introduction

Daily patterns in behavior and physiology are coordinated by circadian pacemakers, which allow organisms to anticipate environmental cycles such as light-dark (Pittendrigh, 1960; Hut and Beersma, 2011). In mammals, the hypothalamic suprachiasmatic nucleus (SCN) is a master circadian pacemaker consisting of approximately 20,000 neurons. Individual cells can generate circadian rhythms via a negative feedback loop involving core clock genes including *Per2* (Hastings et al., 2014; Takahashi, 2016). How and when these rhythms arise during development is not known.

In mice, SCN neurogenesis occurs between embryonic days 10-15 (termed E10-15, where E1 is the day when a vaginal plug is detectable), peaking between E12-14 and forming from ventrolateral to dorsomedial (Shimada and Nakamura, 1973; Kabrita and Davis, 2008; Shimogori et al., 2010). Transcription factors such as *Lhx1*, *Shh*, *Six3*, and *Six6* participate in the embryonic specification of SCN lineages (Shimogori et al., 2010; VanDunk et al., 2011; Clark et

al., 2013; Bedont et al., 2014). However, the markers of terminal differentiation and synaptogenesis peak postnatally (Moore and Bernstein, 1989; Shimogori et al., 2010). The rat SCN has fetal day-night differences in 2-deoxyglucose uptake in vivo around E19, in vivo daily oscillations in clock genes including *Per2* by E20-E21 and in vitro cycling of electrical activity on the day of birth (E22; (Reppert and Schwartz, 1983, 1984; Shibata and Moore, 1987; Sládek et al., 2004; Kovácikova et al., 2006; Houdek and Sumová, 2014). The mouse SCN has detectable fetal daily rhythms in *Per1* transcript levels at E17, and PER1 and PER2 proteins by E18 *in vivo* (Shimomura et al., 2001; Ansari et al., 2009). It is not clear if these results reflect diurnal rhythms imposed by the mother in utero. Recent studies *in vitro* have found daily expression of the PERIOD2::LUCIFERASE (*Per2^{Luc}*) bioluminescent reporter in the whole SCN as early as E13 (Landgraf et al., 2015) or E15 (Wreschnig et al., 2014). It is unclear, however, if or when individual cells in the fetal SCN begin to oscillate and to synchronize their daily rhythms to each other.

To drive coherent rhythms in behavior, cells within the SCN must synchronize their genetic oscillations to an identical period and a consistent phase relationship (Mohawk and Takahashi, 2011; Herzog et al., 2015; Evans and Gorman, 2016). Vasoactive intestinal polypeptide (VIP) is required for normal synchrony in the SCN. Daily addition of VIP entrains SCN neurons, and the absence of VIP or its receptor, VPAC2R, reduces synchrony between neurons and consequently eliminates many daily rhythms (Harmar et al., 2002; Colwell et al., 2003; Aton et al., 2005; Maywood et al., 2006; Ciarleglio et al., 2009). It is not known which intercellular signals underlie circadian synchrony during development (Wang et al., 2014; Ono et al., 2016). In this study, we examined the embryonic onset of endogenous SCN circadian oscillation and intercellular synchrony.

Methods

Animals. All mice were maintained on a C57BL/6JN background (WT) and housed in a 7am-7pm light-dark cycle in the Danforth Animal Facility at Washington University. The *Per2^{Luc}* mouse line was generated by replacing the endogenous mouse *Period2* gene locus with a *Per2^{Luc}* reporter construct (Yoo et al., 2004). For immunochemistry, we compared male and female homozygous *Per2^{Luc}* pups to Vip^{-/-} and Vipr2^{-/-} pups as negative controls. Vaginal plugs confirmed overnight mating of each female. We designated the morning after mating as embryonic day 0.5 (E0.5) and the day of birth as postnatal age 0 (P0). All procedures were approved by the Animal Care and Use Committee of Washington University and followed National Institutes of Health guidelines.

Cultures and Bioluminescence Recording. Pregnant mice were euthanized with CO_2 and cervical dislocation and their embryos dissected into 4 °C Hanks Buffered Saline Solution (Sigma). All surgeries started at 1:00 pm (Zeitgeber Time, ZT 06). We recorded bioluminescence from 300 μm coronal SCN slices from fetal (E13.5-E15.5 and E17.5) and postnatal (P2) homozygous *Per2^{Luc}* mice (Landgraf et al., 2015). Briefly, brains were embedded in a block of 4% low-melting agarose and prepared with a vibraslicer. SCN were dissected with scalpels from sections of the ventral hypothalamus and placed on 0.4 mm membrane inserts (Millipore) in sealed 35 mm Petri dishes (BD Biosciences) with 1ml Dulbecco's Modified Eagle Medium (Sigma, pH 7.2), supplemented with 25 U/ml penicillin, 25 μg/ml streptomycin (Invitrogen), 10 mM HEPES (Sigma), 2% B27 (Invitrogen), 0.35 g/L $NaHCO_3$ (Sigma) and 0.15 mM beetle luciferin (Promega). SCN explants were transferred to a light-tight incubator at 36°C (Onyx, Stanford Photonics). We collected images (XR Mega-10AW camera, Stanford Photonics) every 6 min (6 sec exposure) and then summed every 10 frames with ImageJ software

4

(http://rsbweb.nih.gov/ij) to provide one image every hour. We applied adjacent frame minimization to each movie to filter out bright noise caused by the camera or cosmic rays.

Data Analysis. We analyzed the $Per2^{Luc}$ rhythms of the developing SCN at the level of the whole tissue and with 30μm (pixel) resolution. The statistical analysis for each experiment is described in detail in its respective section. We assessed rhythms measured as the integrated intensity of the SCN tissue with cosinor analysis (software generous gift of B. Meier and A. Kramer). We performed a pixel-based analysis of the same SCN movies. We excluded movies if the corners of the SCN slice moved (3 slices excluded at each of E15.5, 17.5 and P2). We measured periodicity of each pixel (1px= 900μm^2) and defined pixels as circadian if they had a dominant period between 18-32h (P < 0.05 by Lomb-Scargle periodogram analysis (Ruf, 1999)); or a correlation coefficient greater than 0.6 in cosinor analysis. Because the two methods yielded 90 ± 0.02 % (mean ± S.E.; n=30 brains) agreement in pixel classification, we reported results from the periodogram analysis only. The cycle to cycle variability in $Per2^{Luc}$ was evaluated by detrending rhythmic cells with a discrete wavelet transform (Leise, 2015) keeping only detail coefficients between 16-32h, and measuring the interpeak distance (h) of each cycle. We evaluated the synchronization index using the Kuramato method (Kuramoto, 2003).

A radial distribution of mean peak times was constructed for each SCN to identify the presence of core-shell structure. The time of the initial peak for each pixel was calculated following detrending. A radial distribution of peak times was constructed by binning individual cell peaks based on radial distance from a reference point in the left core. A null distribution of radial peak times was calculated by bootstrapping: reassigning peak time values at random to pixels within each SCN and recalculating the radial distribution using 10,000 bootstrap runs. The SCN was determined to have core-shell structure if the radial peak time distribution showed

significant ($P < 0.05$) peaks for the shell region (early-peaking, middle distances) and at least one core region (late-peaking, near and far distances).

Software. Data analysis was performed in the Python language, using packages scipy and numpy (Jones et al., 2014), PyWavelets, Statsmodels (Seabold and Perktold, 2010), and Matplotlib (Hunter, 2007). Parallelization of data processing was achieved via iPython (Pérez and Granger, 2007). Code for data processing is available upon request.

Immunocytochemistry. Brains of mice from ages E13.5-E17.5, P0 and P2 were removed and fixed in 4% paraformaldehyde in phosphate buffered saline (PBS) overnight at 4°C. We transferred them to 30% sucrose in PBS for 24 h at 4°C and sectioned in 30 μm thick coronal slices onto microscope slides. The sections were incubated for 1 h at 4°C in a blocking solution (10% not fat dry milk, 10% bovine serum albumin and 0.3% TritonX-100 in PBS) and then for 48h at 4°C in an anti-VIP (1:1000, Imunostar) or anti-VPAC2R (1:1000, Abcam) rabbit polyclonal antibody diluted in 3% BSA and 0.35% TritonX-100 in PBS. After washing in PBS, the slides next were incubated at room temperature in a biotinylated goat anti-rabbit IgG (1:200; Vector) for 2 h and then ABC solution (1:200; Vectastain Elite ABC Kit, Vector) for 2 h. Finally, we incubated each slide in 50 mM Tris-HCl using 3,3-diaminobenzidine kit (Sigma). After each step, we rinsed 3 times for 15 minutes in PBS. Mounted sections were dehydrated through a series of ethanol and xylene washes. Slides were imaged (NanoZoomer microscope, Leica) and the integrated optical density of the SCN was measured using ImageJ software (Schneider et al., 2012).

Drug Treatments. All drugs were diluted in deionized water and they remained in the recording medium throughout the entire recording without further medium changes. VIP antagonist (200nM PG-99465) provided by Dr. P. Robberecht (Cutler et al., 2003), GABA

antagonist (100µM Gabazine, TROCRIS), MEC (10µM Meclofenamic acid, SIGMA), or TTX (2.5 µM tetrodotoxin).

Results

SCN cells become reliable circadian oscillators after E14.5

Recent *in vitro* studies have demonstrated the presence of circadian rhythms in PER2 expression in whole SCN explants at E13 (Landgraf et al., 2015) or E15 (Wreschnig et al., 2014), around the times of peak or completed neurogenesis, respectively. To test if cell-autonomous oscillations appear prior to tissue-level rhythms, we imaged bioluminescence in fetal *Per2^{Luc}/Per2^{Luc}* SCN slices. SCN explanted at E13.5 displayed no tissue-level circadian rhythms (n=8 SCN from 2 litters; Fig. 1). At this stage, the ventricular zone of dorsal hypothalamus expressed high levels of PER2, sometimes in a circadian pattern (n=2 of the 8 slices; Video 1), but the bilateral SCN region had low to no PER2 expression and no circadian rhythms. In contrast, all tissues explanted on E14.5 or later displayed bilateral *Per2^{Luc}* expression in the ventral hypothalamus, corresponding to the SCN. By E14.5, 45% of SCN were circadian (5 of 11 SCN from 4 litters; Fig. 1). Notably, some E14.5 explants (n=4 of 11, Video 2) also displayed no rhythmic *Per2^{Luc}* expression outside the SCN in the ventricular zone of the dorsal hypothalamus. By E15.5, no hypothalamic explants showed high PER2 expression outside the SCN region and nearly all SCN were circadian (Fig. 1; Video 3; n=11 of 12 E15 SCN from 4 litters, 7 of 7 E17 SCN from 2 litters and 5 of 6 P2 SCN from 1 litter). We conclude that PER2 expression is localized to the SCN and becomes circadian on E14.5.

We next developed methods to culture and image the embryonic SCN for at least 5 days. From these movies, we quantified local circadian rhythms where each pixel included

approximately 10 or fewer cells (Fig. 2A-B). We found the fraction of circadian pixels (cells) increased approximately 7-fold from E14.5 (Fig. 2C-D; 0.10 ± 0.07, mean $\pm$ SEM; n=11 SCN from 4 litters) to E15.5 (0.72 ± 0.11; n=9 SCN from 4 litters; *P < 0.05, one-way Kruskal-Wallis H(3)=10.62, with posthoc Tukey's Honestly Significant Difference). Nearly all regions were circadian in SCN explanted on E17.5 (0.96 ± 0.03; n=4 SCN from 2 litters) and postnatal day 2 (P2, 0.97 ± 0.02; n=3 SCN from 1 litter). The developmental increase in the number of circadian regions correlated with an increase in circadian period in the SCN (Fig. 3A-B). We conclude that a small number of SCN cells initiate endogenous circadian rhythmicity by E14.5, and by E15.5 SCN cells are rhythmic throughout the SCN.

To determine the precision of SCN rhythms during development, we measured the cycle-to-cycle difference in period for each pixel within the fetal SCN over three days of the recording. Interestingly the increase in the number of circadian oscillators correlated with an increase in circadian precision (Fig. 3C-D), suggesting that addition of circadian cells lengthens and stabilizes period in the SCN.

The phase wave typical of adult SCN appears around P2

In adults, PER2 expression progresses as a daily wave from dorsal to ventral across the SCN (Yan and Okamura, 2002; Quintero et al., 2003; Yamaguchi et al., 2003; Evans et al., 2011). We examined when this spatiotemporal patterning of circadian expression arises in the SCN. To do so, we identified the times of daily peak PER2 in each pixel of the SCN and tested for spatial organization of expression. We found reliable daily waves of PER2 from the dorsal to ventral SCN by P2, but not at earlier developmental stages (Videos 4 and 5; Fig. 4). We conclude that phase relationships among SCN cells continue to mature after birth.

Onset of synchrony and intercellular communication within the SCN

Synchronous circadian oscillations in the SCN are required to coordinate daily rhythms in behavior (Schwartz et al., 1987; Aton et al., 2005; Ohta et al., 2005). To test how synchrony develops, we measured the cycle-to-cycle variability in period length and the synchrony index (SI), a quantity that ranges from 1.0 (all oscillators peak together) to 0.0 (all cells peak at uniformly different times of day) from five days of recording. We found that synchrony tends to increase between E14.5 (Fig. 5; SI=0.80±0.5, n=6 SCN) and E15.5 (SI=0.87±0.05, n=9 SCN) reaching a maximum around E17.5 (SI=0.91±0.02, n=4) and P2 (SI=0.94±0.02, n=3 SCN (one unilateral due to changes during recording between halves)). Although there is no significant differences in the SI between ages, SI was positively correlated with the fraction of SCN cells displaying daily rhythms, indicating that intercellular synchrony is developed simultaneously with increased endogenously generated cellular oscillation (Fig. 5C).

We next examined the signaling pathways that could enable synchronization of SCN cells starting around E15.5. VIP signaling is necessary for coordinated circadian rhythms among SCN cells and in behavior of adult mice (Harmar et al., 2002; Colwell et al., 2003; Aton et al., 2005; Maywood et al., 2006; Ciarleglio et al., 2009). We measured the levels of VIP, and its cognate receptor, VPAC2R, by immunocytochemistry between days E14.5 and P2 (Fig. 6). We found VIP (12.5±2.3, n=7) and VPAC2R (15.0±5.6 relative optical density (ROD), n=6) were detectable postnatally above baseline (immunolabeling in the P2 SCN of Vip$^{-/-}$ =2.1±0.7 ROD, n=5 brains and Vipr2$^{-/-}$ =3.8±2.1 ROD, n=5, mean±SEM), but not earlier stages. To further explore this surprising result, we found that a VIP antagonist did not affect synchrony of the E15.5 SCN (Fig. 7). Consistent with prior publications, we found that addition of the VPAC2R antagonist reduced the fraction of circadian cells in the isolated adult SCN to 30% from 84%

(n=1 adult SCN; Cutler et al., Aton et al, 2005). We conclude that VIP and its receptor VPAC2R appear in the SCN after the initiation of circadian rhythms and are not required for circadian synchrony among embryonic SCN cells.

We then performed further pharmacological experiments to test if GABA and/or gap junctions, other candidate coupling mechanisms, might drive synchrony in the SCN before VIP expression begins. Remarkably, antagonists against either or both GABA and gap junctions did not reduce the synchrony index of the E15.5 SCN (Fig. 7).

Discussion

Our results indicate that E15.5 is a critical time in the maturation of the SCN. Real-time imaging revealed that the clock gene, PER2, appears on E14.5 in the SCN and approximately 10% of SCN cells are weakly circadian. By E15.5, nearly all cells within the SCN develop precise circadian rhythms. The cells of the E15.5 SCN are thus competent circadian oscillators. Previous work related this age with the end of neurogenesis (Shimada and Nakamura, 1973; Kabrita and Davis, 2008; Shimogori et al., 2010). At this age the expression of transcription factors as Lhx1 and RORα have a wider distribution across the SCN (VanDunk et al., 2011). Interestingly, RORα is a positive regulator of *Bmal1* expression (Sato et al., 2004), *Bmal1* is an essential transcription factor in circadian rhythmogenesis and activator of *Per* gene expression (Hastings et al., 2014; Takahashi, 2016). In adults, RORα knockouts showed slight behavioral abnormalities in circadian rhythms. We therefore hypothesize that cell autonomous expression of RORα or another factor at E15.5 induces the onset of widespread, sustained circadian oscillations in SCN cells.

Studies using stem cells showed gradual development of circadian oscillations after inducing differentiation with retinoic acid (Yagita et al., 2010; Inada et al., 2014), suggesting that circadian rhythms can be initiated without direct maternal input early during differentiation. Consistent with a prior publication (Landgraf et al., 2015), we found little to no evidence that SCN cells become circadian spontaneously *in vitro*. For example, SCN explanted on 13.5 were arrhythmic and did not show an increase in the fraction of rhythmic pixels over the course of the experiment. SCN isolated at E14.5 or E15.5 similarly did not show changes in the amplitude, period, variability or fraction of circadian cells during 7-day recording. Although we cannot rule out that arrhythmic, fetal SCN cells cultured longer than 7 days might develop daily cycling, our results indicate that the transition from arrhythmic to circadian is rapid and likely requires signals from outside the fetal SCN.

We found no circadian rhythms at E13.5, a small fraction of cells expressed noisy circadian rhythms at E14.5 and nearly all cells were circadian by E15.5. Notably, we found that PER2 was first expressed outside the SCN. At E14.5, extra-SCN PER2 expression was high and occasionally circadian. This extra-SCN expression diminishes by E15.5. It is not clear whether these cells move into the SCN or remain in the dorsal hypothalamus while reducing their PER2 expression. Inclusion of these extra-SCN regions in explants could explain the discrepancy between the two studies that reported the onset of PER2 daily oscillations in hypothalamic explants at E13 or E15 (Wreschnig et al., 2014; Landgraf et al., 2015). Importantly, the correlations in the increasing fraction of rhythmic cells, increasing circadian period and increasing inter- and intracellular period precision during this time could reflect the consequences of cell-cell communication (Webb et al., 2009) and/or maturation of molecular components for circadian rhythm generation (VanDunk et al., 2011; Ono et al., 2016). Previous

studies demonstrated that embryonic SCN have a strong phase-setting in response to perturbations such as surgical isolation (Wreschnig et al., 2014; Landgraf et al., 2015). Together, these data suggest that SCN cells become intrinsically circadian between E14.5 and E15.5. **The presence of a functional circadian clock early in development may indicate the importance of precisely coordinating processes in the fetus such as cell division and differentiation which are adversely affected in *Clock* mutant mice (Du Pré et al., 2014; Inada et al., 2014; Kobayashi et al., 2015)**

The SCN in adult mice displays a dorsal to ventral phase wave in clock gene expression (Yan and Okamura, 2002; Quintero et al., 2003; Yamaguchi et al., 2003; Evans et al., 2011). Because this phase wave is not a fixed property (e.g. can adopt a different pattern after a temperature manipulation in vitro (Jeong et al., 2016), it is important to consider whether the results from the isolated SCN reflect its *in vivo* circadian properties. Critically, our results indicate that under constant conditions, the SCN phase wave first appears after birth. Because we isolated SCN at the same time of day, regardless of developmental age, we conclude that, although surgery can alter circadian phase (Wreschnig et al., 2014; Landgraf et al., 2015), it is unlikely to initiate rhythms in the fetal SCN or the spatial wave seen in the more mature SCN. This postnatal maturation of this SCN network likely involves synaptogenesis which begins around P2 when we found the onset of the phase wave (Bedont and Blackshaw, 2015). It will be intriguing to map the synaptic network topology that contributes to the phase relationships among SCN cells (Abel et al., 2016; Buijink et al., 2016).

Though the network continues to mature after birth, we found that intercellular synchrony is achieved much earlier. A prior report found that surgery can reset rhythms in the fetal SCN (Landgraf et al., 2015). Here, we found that synchrony of E14.5 and immature E15.5 SCN

decreased over the recording, indicating weak or no synchronization between cells. Previous studies also relate an increase in the period variability with a loss of synchrony between cells (Honma et al., 2004; Webb et al., 2009). Our data showed an increase in synchrony by E15.5 (Fig. 5) corresponding to a decrease in cycle-to-cycle period variability, supporting this hypothesis. In adults, VIP and its receptor VPAC2R play a critical role in synchronizing oscillators in the SCN (Harmar et al., 2002; Colwell et al., 2003; Aton et al., 2005; Maywood et al., 2006; Ciarleglio et al., 2009). Although the expression of VIP mRNAs has been detected at E18 in rat (Ban et al., 1997; Houdek and Sumová, 2014) and VIP protein expression has been studied during postnatal ages (Herzog et al., 2000), our results show that the protein is not detectable by immunochemistry before birth. Interestingly, embryonic SCN explants from mice lacking VIP maintain circadian oscillations at the tissue level (Wreschnig et al., 2014). Moreover, our results demonstrate that synchrony occurs at E15.5, before the expression of VIP or receptor VPAC2R. That the exogenous application of VIP antagonist does not decrease synchrony suggests that other signals are likely involved in sustaining synchrony before the presence of VIP. **There is evidence that dopamine, melatonin, or rhythmic feeding may be involved in establishing synchrony between the mother and fetal SCN to coordinate rhythmic cellular processes (Davis and Mannion, 1988; Weaver and Reppert, 1989; Viswanathan et al., 1994). The dopamine pathway in particular merits further investigation as a potential mechanism driving synchrony in the fetal SCN.**

The increase in synchrony in the SCN at E15.5 does coincide with Lhx1 expression across the SCN (VanDunk et al., 2011). This transcription factor is important for the expression of diverse neuropeptide coupling signals aside from VIP, such as GRP or AVP (Bedont et al., 2014). Because these signals can mediate the synchrony in adults (Brown et al., 2005; Maywood

et al., 2011) and in postnatal ages (Ono et al., 2016), they are candidates for mediating SCN synchrony in embryonic development. In rats the first synapses appear in perinatal ages and the sharp increase between P4-P10 (Moore and Bernstein, 1989) suggests that other mechanisms could mediate synchrony prior to synapse formation. Gap junctions have recently been shown to not contribute to circadian synchrony in the adult SCN (Welsh 2017). Our results with a blocker of gap junctions further indicates that they do not play a role in establishing synchrony during SCN development. We conclude that cellular circadian oscillations occur simultaneously with the onset of synchrony by unknown mechanisms.

References

Abel JH, Meeker K, Granados-Fuentes D, John PC, Wang TJ, Bales BB, Doyle FJ, Herzog ED, Petzold LR (2016) Functional network inference of the suprachiasmatic nucleus. Proceedings of the National Academy of Sciences 113:4512-4517.

Ansari N, Agathagelidis M, Lee C, Korf H-WW, von Gall C (2009) Differential maturation of circadian rhythms in clock gene proteins in the suprachiasmatic nucleus and the pars tuberalis during mouse ontogeny. The European journal of neuroscience 29:477-489.

Aton SJ, Colwell CS, Harmar AJ, Waschek J, Herzog ED (2005) Vasoactive intestinal polypeptide mediates circadian rhythmicity and synchrony in mammalian clock neurons. Nature neuroscience 8:476-483.

Ban Y, Shigeyoshi Y, Okamura H (1997) Development of vasoactive intestinal peptide mRNA rhythm in the rat suprachiasmatic nucleus. The Journal of neuroscience : the official journal of the Society for Neuroscience 17:3920-3931.

Bedont JL, Blackshaw S (2015) Constructing the suprachiasmatic nucleus: a watchmaker's perspective on the central clockworks. Frontiers in Systems Neuroscience 9.

Bedont JL, LeGates TA, Slat EA, Byerly MS, Wang H, Hu J, Rupp AC, Qian J, Wong GW, Herzog ED, Hattar S, Blackshaw S (2014) Lhx1 controls terminal differentiation and circadian function of the suprachiasmatic nucleus. Cell reports 7:609-622.

Brown TM, Hughes AT, Piggins HD (2005) Gastrin-releasing peptide promotes suprachiasmatic nuclei cellular rhythmicity in the absence of vasoactive intestinal polypeptide VPAC2 receptor signaling. The Journal of neuroscience 25:11155-11164.

Buijink RM, Almog A, Wit CB, Roethler O, Engberink AHO, Meijer JH, Garlaschelli D, Rohling JHT, Michel S (2016) Evidence for Weakened Intercellular Coupling in the Mammalian Circadian Clock under Long Photoperiod. PloS one 11.

Ciarleglio CM, Gamble KL, Axley JC, Strauss BR, Cohen JY, Colwell CS, McMahon DG (2009) Population encoding by circadian clock neurons organizes circadian behavior. The Journal of neuroscience : the official journal of the Society for Neuroscience 29:1670-1676.

Clark DD, Gorman MR, Hatori M (2013) Aberrant development of the suprachiasmatic nucleus and circadian rhythms in mice lacking the homeodomain protein Six6. J Biol Rhythms 28:15-25.

Colwell CS, Michel S, Itri J, Rodriguez W, Tam J, Lelievre V, Hu Z, Liu X, Waschek JA (2003) Disrupted circadian rhythms in VIP- and PHI-deficient mice. American journal of physiology Regulatory, integrative and comparative physiology 285:R939-R949.

Cutler DJ, Haraura M, Reed HE, Shen S, Sheward JW, Morrison CF, Marston HM, Harmar AJ, Piggins HD (2003) The mouse VPAC2 receptor confers suprachiasmatic nuclei cellular rhythmicity and responsiveness to vasoactive intestinal polypeptide in vitro. European Journal of Neuroscience 17:197-204.

Davis FC, Mannion J (1988) Entrainment of hamster pup circadian rhythms by prenatal melatonin injections to the mother. The American journal of physiology 255:48.

Du Pré BC, Van Veen TA, Young ME, Vos MA, Doevendans PA, Van Laake LW (2014) Circadian rhythms in cell maturation. Physiology (Bethesda, Md) 29:72-83.

Evans JA, Gorman MR (2016) In synch but not in step: Circadian clock circuits regulating plasticity in daily rhythms. Neuroscience 320:259-280.

Evans JA, Leise TL, Castanon-Cervantes O, Davidson AJ (2011) Intrinsic regulation of spatiotemporal organization within the suprachiasmatic nucleus. PloS one 6.

Harmar AJ, Marston HM, Shen S, Spratt C, West KM, Sheward WJ, Morrison CF, Dorin JR, Piggins HD, Reubi JC, Kelly JS, Maywood ES, Hastings MH (2002) The VPAC(2) receptor is essential for circadian function in the mouse suprachiasmatic nuclei. Cell 109:497-508.

Hastings MH, Brancaccio M, Maywood ES (2014) Circadian pacemaking in cells and circuits of the suprachiasmatic nucleus. Journal of neuroendocrinology 26:2-10.

Herzog ED, Kiss IZZ, Mazuski C (2015) Measuring synchrony in the mammalian central circadian circuit. Methods in enzymology 552:3-22.

Herzog ED, Grace MS, Harrer C, Williamson J, Shinohara K, Block GD (2000) The role of Clock in the developmental expression of neuropeptides in the suprachiasmatic nucleus. The Journal of comparative neurology 424:86-98.

Honma S, Nakamura W, Shirakawa T, Honma K-i (2004) Diversity in the circadian periods of single neurons of the rat suprachiasmatic nucleus depends on nuclear structure and intrinsic period. Neuroscience Letters 358:173176.

Houdek P, Sumová A (2014) In Vivo Initiation of Clock Gene Expression Rhythmicity in Fetal Rat Suprachiasmatic Nuclei. PLoS ONE 9.

Hunter JD (2007) Matplotlib: A 2D Graphics Environment. Computing in Science & Engineering 9:90-95.

Hut RA, Beersma DGM (2011) Evolution of time-keeping mechanisms: early emergence and adaptation to photoperiod. Philosophical Transactions of the Royal Society of London B: Biological Sciences 366:2141-2154.

Inada Y, Uchida H, Umemura Y, Nakamura W, Sakai T, Koike N, Yagita K (2014) Cell and tissue-autonomous development of the circadian clock in mouse embryos. FEBS Letters.

Jeong B, Hong JH, Kim H, Choe HK, Kim K, Lee KJ (2016) Multi-stability of circadian phase wave within early postnatal suprachiasmatic nucleus. Scientific reports 6:21463.

Jones E, Oliphant T, Peterson P (2014) {SciPy}: open source scientific tools for {Python}. {SciPy}: open source scientific tools for {Python}.

Kabrita CS, Davis FC (2008) Development of the mouse suprachiasmatic nucleus: determination of time of cell origin and spatial arrangements within the nucleus. Brain research 1195:20-27.

Kobayashi Y, Ye Z, Hensch TK (2015) Clock genes control cortical critical period timing. Neuron 86:264-275.

Kováciková Z, Sládek M, Bendová Z, Illnerová H, Sumová A (2006) Expression of clock and clock-driven genes in the rat suprachiasmatic nucleus during late fetal and early postnatal development. J Biol Rhythms 21:140-148.

Kuramoto Y (2003) Chemical Oscillations, Waves, and Turbulence: Dover Publications.

Landgraf D, Achten C, Dallmann F, Oster H (2015) Embryonic development and maternal regulation of murine circadian clock function. Chronobiology International 32.

Leise TL (2015) Wavelet-based analysis of circadian behavioral rhythms. Methods in enzymology 551:95-119.

Maywood ES, Chesham JE, O'Brien JA, Hastings MH (2011) A diversity of paracrine signals sustains molecular circadian cycling in suprachiasmatic nucleus circuits. Proceedings of the National Academy of Sciences of the United States of America 108:14306-14311.

Maywood ES, Reddy AB, Wong GK, O'Neill JS, O'Brien JA, McMahon DG, Harmar AJ, Okamura H, Hastings MH (2006) Synchronization and maintenance of timekeeping in suprachiasmatic circadian clock cells by neuropeptidergic signaling. Current biology 16:599-605.

Mohawk JA, Takahashi JS (2011) Cell autonomy and synchrony of suprachiasmatic nucleus circadian oscillators. Trends in neurosciences 34:349-358.

Moore RY, Bernstein ME (1989) Synaptogenesis in the rat suprachiasmatic nucleus demonstrated by electron microscopy and synapsin I immunoreactivity. The Journal of neuroscience : the official journal of the Society for Neuroscience 9:2151-2162.

Ohta H, Yamazaki S, McMahon DG (2005) Constant light desynchronizes mammalian clock neurons. Nature Neuroscience 8:267-269.

Ono D, Honma S, Honma K-I (2016) Differential roles of AVP and VIP signaling in the postnatal changes of neural networks for coherent circadian rhythms in the SCN. Science advances 2.

Pérez F, Granger BE (2007) IPython: a system for interactive scientific computing. Computing in Science & Engineering.

Pittendrigh CS (1960) Circadian Rhythms and the Circadian Organization of Living Systems. Cold Spring Harbor Symposia on Quantitative Biology 25:159-184.

Quintero JE, Kuhlman SJ, McMahon DG (2003) The biological clock nucleus: a multiphasic oscillator network regulated by light. Journal of Neuroscience 23:8070-8076.

Reppert SM, Schwartz WJ (1983) Maternal coordination of the fetal biological clock in utero. Science (New York, NY) 220:969-971.

Reppert SM, Schwartz WJ (1984) The suprachiasmatic nuclei of the fetal rat: characterization of a functional circadian clock using 14C-labeled deoxyglucose. The Journal of neuroscience 4.

Ruf T (1999) The Lomb-Scargle periodogram in biological rhythm research: analysis of incomplete and unequally spaced time-series. Biological Rhythm Research 30:178-201.

Sato TK, Panda S, Miraglia LJ, Reyes TM, Rudic RD, McNamara P, Naik KA, FitzGerald GA, Kay SA, Hogenesch JB (2004) A functional genomics strategy reveals Rora as a component of the mammalian circadian clock. Neuron 43:527-537.

Schneider CA, Rasband WS, Eliceiri KW (2012) NIH Image to ImageJ: 25 years of image analysis. Nature Methods 9:671-675.

Schwartz WJ, Gross RA, Morton MT (1987) The suprachiasmatic nuclei contain a tetrodotoxin-resistant circadian pacemaker. Proceedings of the National Academy of Sciences of the United States of America 84:1694-1698.

Seabold S, Perktold J (2010) Statsmodels: Econometric and statistical modeling with python. Proceedings of the 9th Python in Science ….

Shibata S, Moore RY (1987) Developm ent of neuronal activity in the rat suprachiasmatic nucleus. Developmental Brain Research 34.

Shimada M, Nakamura T (1973) Time of neuron in mouse hypothalamic nuclei. Experimental Neurology 41:163-173.

Shimogori T, Lee DA, Miranda-Angulo A, Yang Y, Wang H, Jiang L, Yoshida AC, Kataoka A, Mashiko H, Avetisyan M, Qi L, Qian J, Blackshaw S (2010) A genomic atlas of mouse hypothalamic development. Nature Neuroscience 13:767-775.

Shimomura H, Moriya T, Sudo M, Wakamatsu H, Akiyama M, Miyake Y, Shibata S (2001) Differential daily expression of Per1 and Per2 mRNA in the suprachiasmatic nucleus of fetal and early postnatal mice. The European journal of neuroscience 13:687-693.

Sládek M, Sumová A, Kováciková Z, Bendová Z, Laurinová K, Illnerová H (2004) Insight into molecular core clock mechanism of embryonic and early postnatal rat suprachiasmatic nucleus. Proceedings of the National Academy of Sciences of the United States of America 101:6231-6236.

Takahashi JS (2016) Transcriptional architecture of the mammalian circadian clock. Nature Reviews Genetics 18:164-179.

VanDunk C, Hunter LA, Gray PA (2011) Development, Maturation, and Necessity of Transcription Factors in the Mouse Suprachiasmatic Nucleus. The Journal of Neuroscience 31:6457-6467.

Viswanathan N, Weaver DR, Reppert SM, Davis FC (1994) Entrainment of the fetal hamster circadian pacemaker by prenatal injections of the dopamine agonist SKF 38393. The Journal of neuroscience : the official journal of the Society for Neuroscience 14:5393-5398.

Wang M-HH, Chen N, Wang J-HH (2014) The coupling features of electrical synapses modulate neuronal synchrony in hypothalamic superachiasmatic nucleus. Brain research 1550:9-17.

Weaver DR, Reppert SM (1989) Periodic feeding of SCN-lesioned pregnant rats entrains the fetal biological clock. Developmental Brain Research 46:291-295.

Webb AB, Angelo N, Huettner JE, Herzog ED (2009) Intrinsic, nondeterministic circadian rhythm generation in identified mammalian neurons. Proceedings of the National Academy of Sciences of the United States of America 106:16493-16498.

Wreschnig D, Dolatshad H, Davis FC (2014) Embryonic Development of Circadian Oscillations in the Mouse Hypothalamus. J Biol Rhythms 29:299-310.

Yagita K, Horie K, Koinuma S, Nakamura W, Yamanaka I, Urasaki A, Shigeyoshi Y, Kawakami K, Shimada S, Takeda J, Uchiyama Y (2010) Development of the circadian oscillator during differentiation of mouse embryonic stem cells in vitro. Proceedings of the National Academy of Sciences of the United States of America 107:3846-3851.

Yamaguchi S, Isejima H, Matsuo T, Okura R, Yagita K, Kobayashi M, Okamura H (2003) Synchronization of Cellular Clocks in the Suprachiasmatic Nucleus. Science 302:1408-1412.

Yan L, Okamura H (2002) Gradients in the circadian expression of Per1 and Per2 genes in the rat suprachiasmatic nucleus. European Journal of Neuroscience 15:1153-1162.

Yoo S-H, Yamazaki S, Lowrey PL, Shimomura K, Ko CH, Buhr ED, Siepka SM, Hong H-K, Oh W, Yoo O, Menaker M, Takahashi JS (2004) PERIOD2::LUCIFERASE real-time reporting of circadian dynamics reveals persistent circadian oscillations in mouse peripheral tissues. Proceedings of the National Academy of Sciences of the United States of America 101:5339-5346.
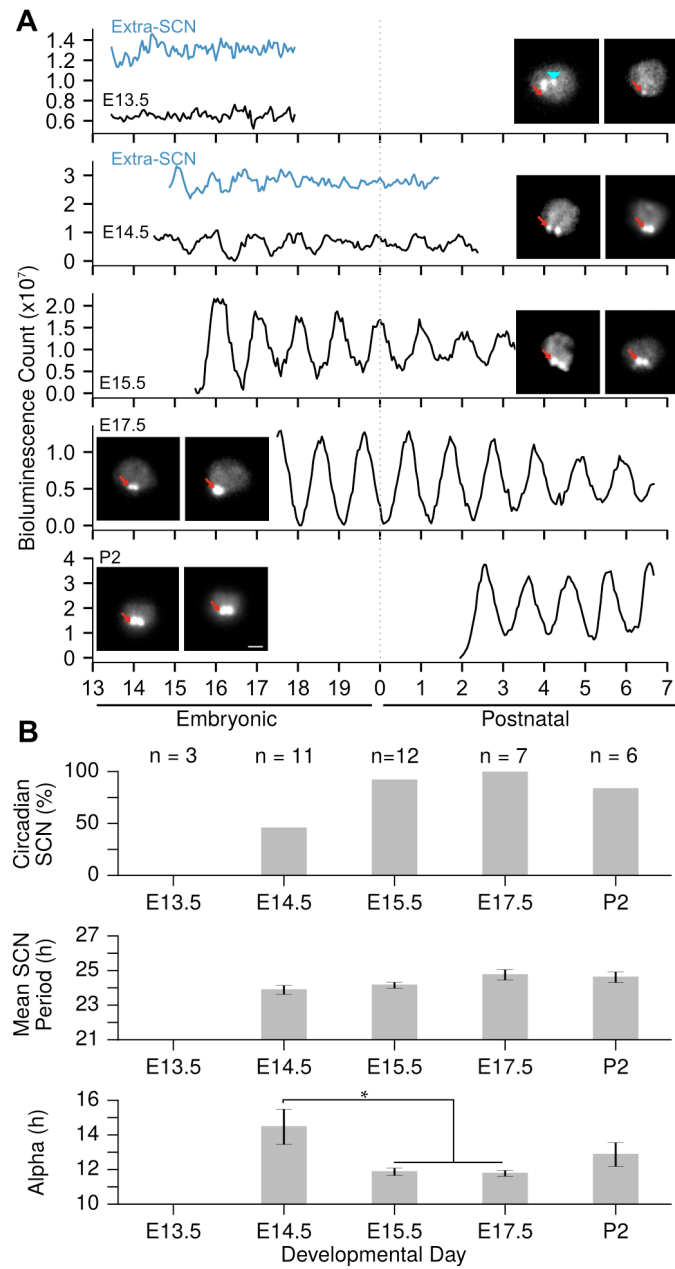
Figure Legends

Figure 1.   Circadian rhythms in the SCN during development. Long-term, real-time

recordings of PER2 expression from SCN harvested after E14.5 showed reliable circadian

periods between 18-32h. (A) Representative records of *Per2^Luc* bioluminescence from SCN

starting on the day they were explanted. Note the weak circadian oscillations that were found in some E14.5 SCN. Insets show images of two representative SCN from each age. Some SCN harvested at E13.5 expressed *Per2^{Luc}* above the SCN region along the ventricular zone of dorsal hypothalamus (blue arrow head, n=5/8). All others harvested at this age and older reliably expressed high levels of PER2 in the bilateral SCN. Scale bar = 10px = 300μm. (B) Nearly all SCN expressed significant circadian rhythms when harvested on or after E15.5 (Upper panel), with periods close to 24 h (mean ± SEM; Middle panel) and durations of daily *Per2^{Luc}* expression above the mean close to 12 h (alpha; mean ± SEM, Lower panel; $P < 0.05$, one-way ANOVA, Tukey's HSD). Note, 8 slices were examined at E13.5, however, we excluded 5 because they did not express detectable PER2 in the SCN region.
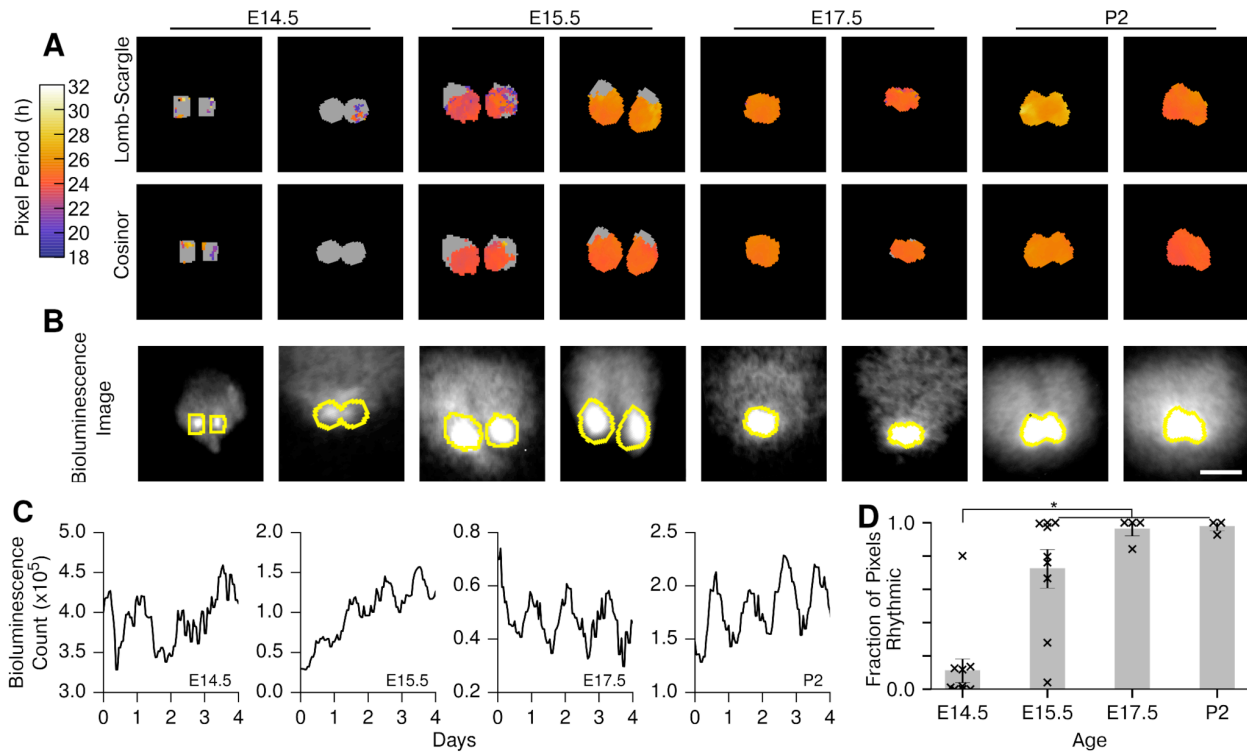
Figure 2. Embryonic SCN cells express PER2 rhythmically beginning around E14.5 in vitro. (A) Heat maps of two SCN explanted at each developmental stage show circadian pixels based on Lomb-Scargle periodogram (power above P < 0.05) and Cosinor analysis (correlation coefficient greater than 0.6). We therefore report results only from periodogram analyses for simplicity. (B) Representative *Per2^Luc^* bioluminescence images of the same SCN explants (1 h integration, 2 x 2 binning). Scale bar = 10px = 300μm. (C) Representative *Per2^Luc^* bioluminescence recordings from single rhythmic pixels from SCN cultured at different embryonic stages. Note the competence of the E15.5 SCN to generate and sustain circadian rhythms in PER2 protein expression. (D) The fraction of circadian pixels in each SCN (mean ± SEM,) was higher for explants at E15.5 and older (* P < 0.05, one-way ANOVA, Tukey's Honestly Significant Difference (HSD), n=at least 3 SCN at each age where age is reported as days post mating, E0.5, and post birth, E20.5=P0).
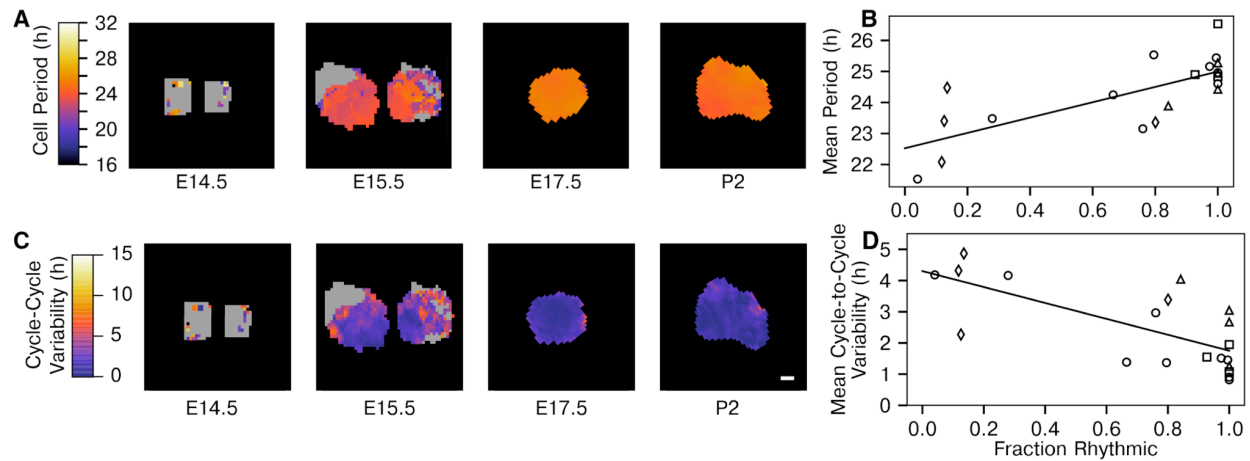
Figure 3. Circadian period and precision of SCN cells increased with development. (A) Heat maps from representative SCN show the mean period over 5 days of recording. (B) The fraction of rhythmic pixels correlated with an increase in the mean SCN period (Least-squares linear regression P = 0.00019, Pearson's r = 0.74. SCN with fewer than 5 circadian pixels were considered arrhythmic and excluded from this analysis. E14.5: diamonds, n=6 of 11, E15.5: circles, n=9 of 9, E17.5: triangles, n=4 of 4, P2: squares, n=3 of 3). (C) Representative mean cycle-to-cycle variability heat maps show the increase in circadian precision with age. Scale bar = 150 μm. (D) The average variability of the daily period across all rhythmic pixels within each isolated SCN inversely correlated with the fraction of circadian cells (least-squares linear regression P = 0.0006, Pearson's r = -0.70; symbols as in B), SCN with fewer than 5 circadian pixels were considered arrhythmic and excluded from this analysis.
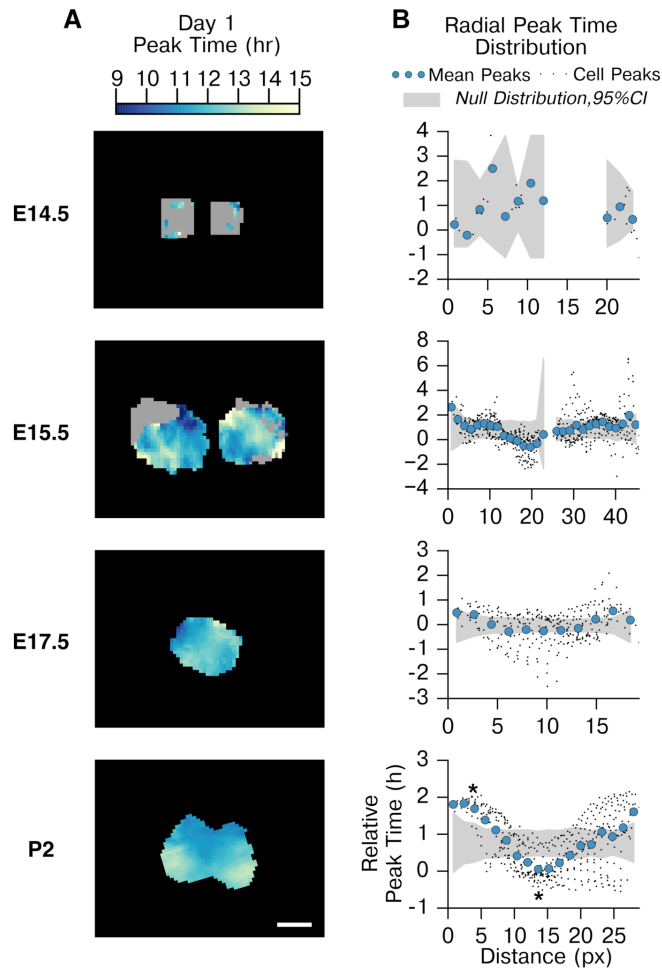
Figure 4. The phase wave of PER2 expression in the SCN appeared only after birth. (A) Heat maps of the time of peak PER2 expression across representative SCN. Note the dorsal-to-ventral distribution across the cells of the P2 SCN. Scale bar = 300 μm. (B) Radial distribution of peak times revealed a core-shell structure in the P2, but not younger, SCN explants. We compared the average differences in the times of peak PER2 expression as a function of distance from the ventral margin of each SCN with a null distribution of randomly shuffled peak times (shaded area=95% CI for mean peak time calculated from 10,000 resamples). At P2, PER2 peaked significantly later in the ventral core than the dorsal shell, as seen in this representative example.
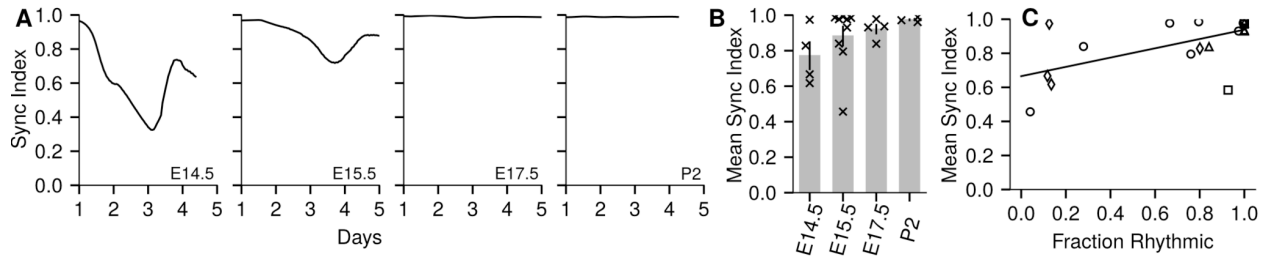
Figure 5. The synchrony between SCN cells increased and became more stable as the fraction of circadian cells increased. (A) Representative traces of the synchronization index (also called the Kuramoto order parameter or Rayleigh Statistic, r) among regions within the cultured SCN at different ages. (B) The average synchronization index of SCN slices (mean ± SEM, 24h excluded from either end of analysis) did not reliably increase with age, but (C) correlated with the fraction of circadian cells in the SCN (symbols as in Figure. 3; Least-squares linear regression P = 0.004, Pearson's r = 0.61, n=at least 3 SCN at each age).
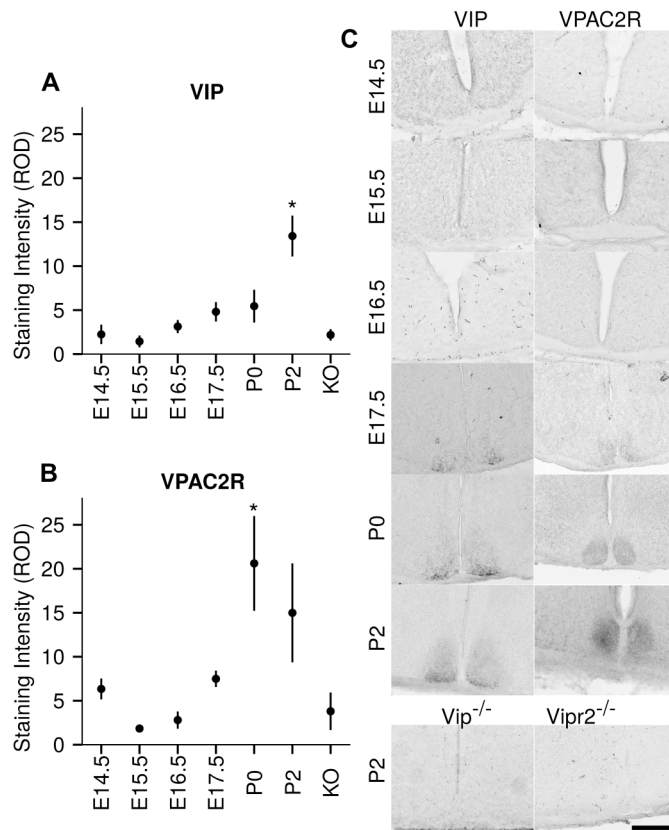
Figure 6. VIP and VPAC2R expression matured in the postnatal SCN. (A) Immunostaining intensity (Mean relative optical density ± SEM, n=9, 5, 7, 6, 7 and 7 brains at each age, respectively) of VIP in the SCN was significant by P2 compared to Vip-knockout controls (n=5, *P < 0.05, one-way ANOVA with Tukey's HSD). (B) Immunostaining intensity (Mean ± SEM) of VPAC2R (n=6, 6, 5, 5, 7, and 6 brains, respectively) was significant by P0 compared to Vipr2-knockout controls (n=5, *P<0.05, one-way ANOVA with Tukey's HSD). (C) Representative coronal SCN sections show the VIP (left panel) and VPAC2R (right panel) immunoreactivity at different ages. Scale bar = 200 μm.
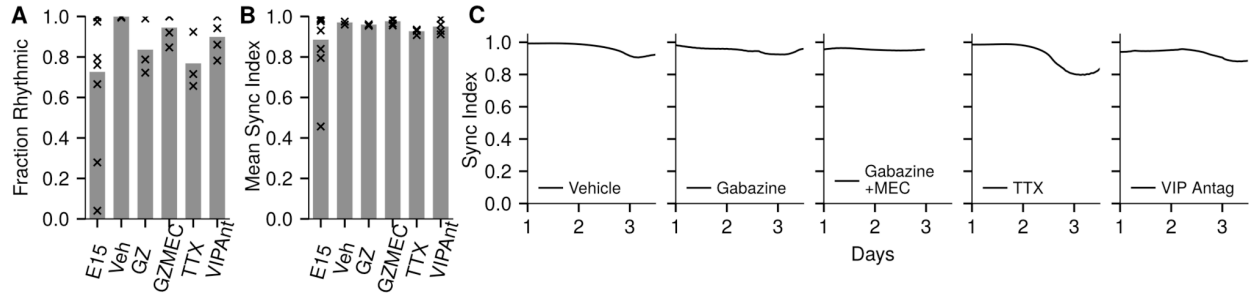
Figure 7. Antagonists of GABA or VIP signaling, gap junctions or neuronal firing did not disrupt circadian synchrony in the developing SCN. Drugs applied during the first day of culture of E15.5 SCN explants did not change (A) the fraction of pixels with circadian $Per2^{Luc}$ (grey bars show the means across all SCN recorded at each developmental stage), or (B) the mean sync index over the 5 days of recording. (C) The synchronization index within a representative cultured E15.5 SCN treated with Veh (Vehicle), Gz (100µM Gabazine), MEC (10µM Meclofenamic acid), VIP antagonist (200nM PG-99465), or TTX (2.5 µM tetrodotoxin).